THE EFFECTS OF MAN-MADE AND CLIMATIC CHANGES ON A TROPICAL COASTAL SYSTEM: A COMPARATIVE STUDY

A THESIS SUBMITTED TO
THE GLOBAL ENVIRONMENTAL SCIENCE
UNDERGRADUATE DIVISION IN PARTIAL FULFILLMENT
OF THE REQUIREMENTS FOR THE DEGREE OF

BACHELOR OF SCIENCE

IN

GLOBAL ENVIRONMENTAL SCIENCE

MAY 2015

By

Camilla Tognacchini

Thesis Advisor

Margaret Anne McManus

I certify that I have read this thesis and that, in my opinion, it is satisfactory in scope and quality as a thesis for the degree of Bachelor of Science in Global Environmental Science.

THESIS ADVISOR

_____

Professor Margaret Anne McManus
Department of Oceanography

ACKNOWLEDGEMENTS

I would like to express my most sincere gratitude to my advisor Margaret McManus for guiding me through this research and for being an awesome inspiration to me. I would also like to thank Kathleen Ruttenberg and Rosie Alegado for assisting me with my research and writing. I could not have done this without all the support from the McManus Lab, the Ruttenberg Lab and the Alegado Lab and all the wonderful people I have worked with. A special thanks to Conor Jerolmon for his patience with helping me through data analysis.

My deepest appreciation goes to my family. I would like to thank my *keiki* Kamaliʻi and Vanina for sharing this adventure with me. And my mother, Iaia, for always being there for me.

The biggest *mahalo* goes to Paepae O Heʻeia and all the amazing work they've done at Heʻeia Fishpond, without which this research would have not been possible.

This work was supported by Hawaii Sea Grant Program Development Project R/HE-24PD "Linking physical variability to the geochemistry and biology of the Heʻeia Fishpond" PIs M.A. McManus and K. Ruttenberg. Grant Award No: NA09OAR4170060. We are grateful for this support.

ABSTRACT

Hawaiian coastal waters have been, and continue to be, subject to major anthropogenic impacts from land use changes, which have altered the characteristics of the coastal environment. This study aims to investigate the effects of perturbations in the physical environment of a semi-enclosed tropical coastal embayment, He‘eia Fishpond. A two-month time series of *in situ* measurements within He‘eia Fishpond captures multiple scales of variability of environmental parameters. Instruments were deployed to observe the effects of invasive mangrove removal, and by fortune, also observed the effects of three tropical storms. We explain the observed environmental variability in terms of local and/or remote forcing, and investigate how physical variability across a range of scales affects in-pond geochemistry and biogeography. As climate change continues to increase sea surface temperatures the frequency of tropical cyclones is projected to increase. It is critical to have an understanding of how increased temperature and rainfall affect our coastal waters. With this understanding, areas like He‘eia Fishpond can be properly managed to mitigate future climate variability.

TABLE OF CONTENTS

Page

LIST OF TABLES

Table Page

LIST OF FIGURES

Figure Page

Figure Page

CHAPTER I. INTRODUCTION

Location

The Heʻeia Fishpond (HFP) is a man-made tropical coastal embayment located in Heʻeia Uli, at the mouth of the Heʻeia watershed (Figure 1). The fishpond (*loko iʻa*) is built on a fringing reef in southern Kāneʻohe Bay. The watershed drains into Heʻeia Stream, which flows into Kāneʻohe Bay adjacent to the northern end of the fishpond. Three small tributaries of Heʻeia stream drain directly into the fishpond. The fishpond is fully enclosed by a semi-permeable *kuapā* (rock wall) that is 1.3 miles long, interspersed with *mākāhā* (gate openings) that allow water exchange with the streams and the adjacent bay (Kāneʻohe Bay) (Figure 2).

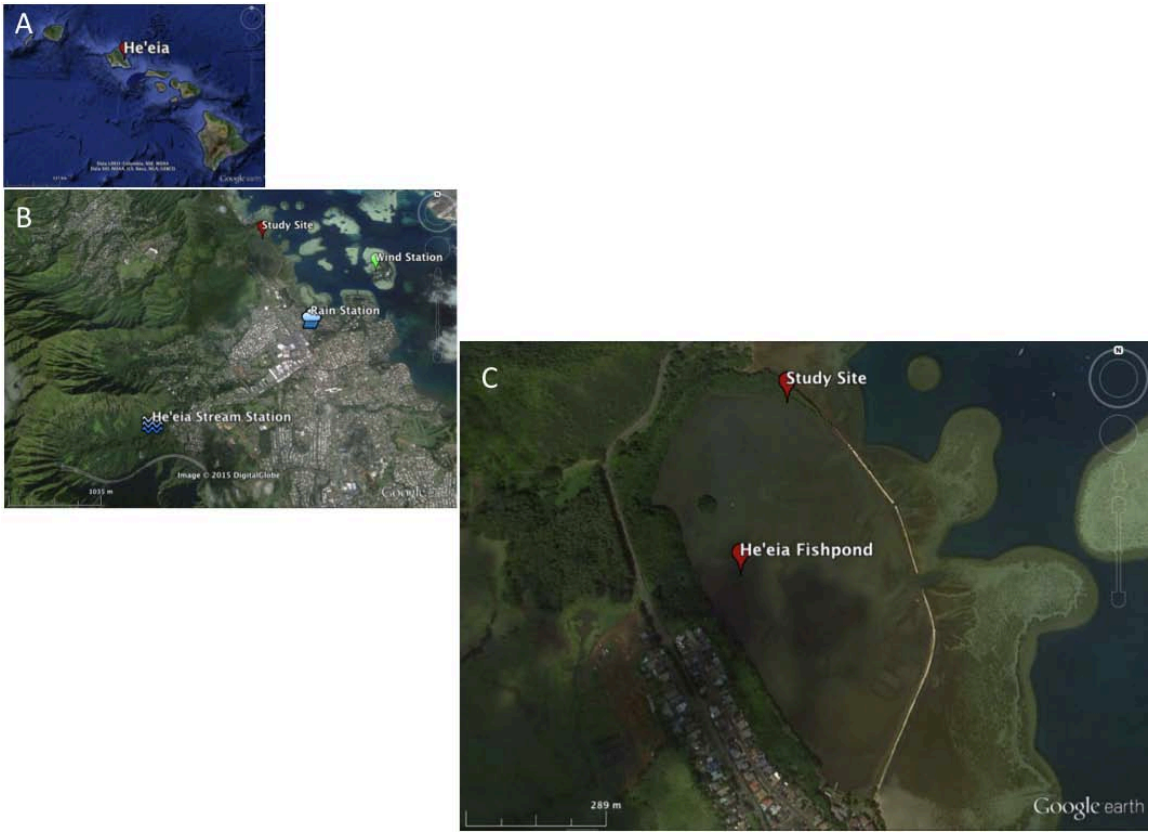

Figure 1. Map of Hawaiʻi and Heʻeia Fishpond. A) The main Hawaiian Islands. B) Map of Heʻeia watershed and Kāneʻohe Bay with location of study site and weather station locations: USGS stream flow station, NOAA rain station and HIMB wind station. C) Map of Heʻeia Fishpond. (Google Earth, 2015)

Characteristics of He‘eia Fishpond

Bathymetry: The fishpond is characterized by a shallow water column (< 2m), with an average depth of 0.38 m at neap low tide, and an average tidal range of 0.72 m.

Figure 2. Map of He‘eia Fishpond and circulation. Location of gate openings, *mākāhā,* and direction of water flow (blue arrows) (Google Earth, 2015).

Tides: The tides ebb and flow through the *mākāhā*: Ocean Mākāhā 1 (OM1), Ocean Mākāhā 2 (OM2), Triple Mākāhā (TM) and Ocean Break (OB) (Figure 2). During neap tide 33% of the water in HFP is exchanged with Kāne‘ohe Bay. During spring tide, 73% of the water in HFP is exchanged with Kāne‘ohe Bay. Water exchange also occurs through 3 river Mākāhā (RM1, RM2, RM3) (Figure 2). The major source of freshwater input is through RM2. The northeastern side of the fishpond experiences the largest water exchange, compared to the rest of the pond due to water exchange mainly through TM and OM1. As a result of inputs from both oceanic and freshwater sources the water in the fishpond is brackish (Timmermann et al., in prep.).

Wind: He‘eia watershed is located on the windward coast of O‘ahu, and is subject to the northeasterly trade winds. HFP is shallow and thus effected by wind driven mixing. Wind speed and direction influence both water movement and water column mixing (Timmermann et al., in prep.). The HFP is too small to be influenced by the Coriolis effect.

Solar heating: The shallow depth of HFP allows for solar radiation to warm the pond so that temperatures are often higher in HFP than in Kāne‘ohe Bay. In absence of wind there is less turbulent mixing and stratification of the water column becomes a dominant force (Timmermann et al., in prep.).

Stratification: The average vertical changes (between surface and deep water) in temperature and salinity throughout the pond are changes in temperature of 0.11^{o} C and changes in salinity of 0.72 PSU. The area of highest stratification is in the northwest portion of the fishpond to the west of the small island (Timmermann et al., in prep.).

Turbidity: The Heʻeia watershed is a steep-sided mountainous watershed subject to episodic rain events. These rain events can cause rapid fluvial discharge within a few hours (Timmerman et al., in prep.). During rain events, the concentration and transport of suspended particulate matter in fluvial discharge increases exponentially with increased stream flow (Hoover and Mackenzie, 2009). The steep mountain slopes in the Heʻeia watershed are physically eroded by the rain and are the main source of fine-grained terrigenous sediments to the coastal ocean. Because Heʻeia fishpond is located at the mouth of the Heʻeia stream, this is where the majority of the sediments arrive. Rain events usually increase sediment loading in coastal systems and account for 80% of the annual load of sediments delivered to the coastal ocean, in Hawaiʻi (Timmerman et al., in prep.). The highest rates of precipitation, fluvial discharge and sediment load occur during storm conditions.

The study site (Figure 2), which is the focus of this thesis, is located in the northeastern corner of HFP near stake 6, which has been characterized in previous studies (Timmermann et al. in prep.). At the initiation of the project the study site was located in an area protected by mangrove canopy cover.

Land use changes in Heʻeia Fishpond

Heʻeia Fishpond is an impressive feat of Native Hawaiian cultural heritage, believed to have been built about *ca.* 800 years ago for the purpose of extensive aquaculture production (Kelly, 1975). The location of the fishpond in an estuarine system allows the system to capture the natural abundance of productivity characteristic of estuarine systems.

Historically the area of Heʻeia watershed was managed traditionally by the native Hawaiians as the Heʻeia *ahupuaʻa*. An *ahupuaʻa* is a watershed-based system of ecosystem management that integrates fresh water and marine water resources in a continuum from the mountains to the sea (Jokiel et al., 2011). Society in pre-contact Hawaiʻi developed as a result of gaining control of water systems for aquaculture and agriculture (Kikuchi, 1976). The earliest records of land use in Kāneʻohe Bay date to 1789 when it was reported to have one of the most extensive taro cultivations (*loʻi*) of the Hawaiian Islands (Devaney, 1976). A combination of socio-economic factors led to the decline of Hawaiian natural resource management practices (Keala et al., 2007) and unsustainable land use practices replaced the sustainable traditional practices of land management (Jokiel et al., 2011).

Mangroves

Land ownership became a reality in Hawai‘i in the 1850s and with it plantation style agriculture in He‘eia, followed by animal grazing and urban development (Kelly, 1975). To control the sediment runoff from agricultural fields, red mangrove (*Rhizopora Mangle)* was introduced to He‘eia in 1922 (Siple and Donahue, 2013). Invasive mangroves in Hawai‘i are considered to be ecosystem engineers by altering the characteristics of the wetland in the intertidal zone (Demopoulos and Smith, 2010). The mangrove habitat, characterized by accumulation and retention of sediment, replaced the native sand flat environment (Siple and Donahue, 2013). Restoration efforts are now underway in He‘eia Fishpond, but mangrove decomposition in Hawai‘i is slow and recovery of the native habitat can take many decades (Siple and Donahue, 2013). The watershed in He‘eia has shifted from sediments being retained on land by reduced water flow through the *lo‘i*, to being discharged into the stream and into the coastal ocean where they accumulate. The fishpond, once built on a coral reef, is now characterized by a fine-grained silty sediment. Invasive mangroves established on the side of the fishpond along the coastline and along the walls of the pond cause a reduction in flow. Reduced flow has led to enhanced accumulation of fine-grained sediment especially in mangrove-forested areas along the stream, has lead to more sediment being trapped and retained within the embayment.

Storm impacts

Kāne‘ohe Bay and He‘eia Fishpond are historically subject to episodic flooding events (Kelly, 1975). In the Kāne‘ohe Bay system, a “storm” is defined as 5.1 cm of rainfall or more over a 24-hour period (Ringuet and Mackenzie 2005). It takes 2 to 9 days for Kāne‘ohe Bay to be restored to ‘normal’ conditions after a storm. The magnitude of tidal exchange and winds determine the length of recovery time, while the magnitude of the storm is less significant (Ringuet and Mackenzie, 2005). The same is true for He‘eia Fishpond, where the tidal stage and wind forcing influence the amount of time it takes for the fishpond to return to ‘normal’ conditions (Timmermann et al., in prep.). Neap tides prolong storm impact on HFP, while spring tides accelerate flushing rates. In light winds the retention time is longer while with stronger winds the flushing is accelerated and recovery time is faster (Timmermann et al., in prep.). On average, it takes 4 days for HFP to be restored to ‘normal’ conditions after a storm (Timmermann et al., in prep.).

Purpose of this study

Using high-resolution data from our physical instrumentation around He‘eia Fishpond and from water column profiling, our goal was to separate the scales of variability in the physical environment, explain each in terms of local and/or remote forcing, and investigate how physical variability across a range of scales affects in-pond geochemistry and biogeography.

CHAPTER II. METHODS

Study Site

He‘eia fishpond is located in southern Kāne‘ohe Bay, in the district of Ko‘olaupoko, on the eastern shore of the Island of O‘ahu, Hawai‘i (Figure 1). The study site is located $21^0$26’32” N, $157^0$48’29” W, in the northeastern corner of He‘eia fishpond adjacent to an invasive mangrove patch (Figure 2). The site is pond ward of the edge of a mangrove patch. The site is also adjacent to a large area where mangroves were previously removed (Figure 3). To the east of the study site is an area of fine-grained sediment, were the mangroves were previously topped off but the roots were left behind and still retain sediment. On the western side of the site is an area fully covered by mangroves (Figure 3). The study area is located within the pond adjacent to a 175 m^2 area of mangroves (Figure 4) targeted for removal during the study. The measured patch of mangrove represents the last stand against the ocean wall in the restoration efforts of mangrove removal.

Figure 3. Aerial view of the study site taken on 16 June 2014. Map of the 175 m^2 mangrove area to be removed (blue triangle), the study site (orange string) and instrument package location (X).

Figure 4. Ground view of a small portion of mangrove patch area to be removed.

Site Survey

An initial site survey was conducted on May 9, 2014 to assess the general circulation conditions in the area where the mangroves would be removed and to determine the best location to deploy instrumentation. The mangrove to be removed encompassed a triangular area measuring 14m x 23m x 10.5 (175m^2) with the long edge facing the pond (Figures 3 and 5). We deployed a Nortek current meter in 4 different locations along this triangular mangrove patch. Three measurements were taken near the edge of the mangrove patch and one current measurement was taken 1.5 m away from the mangrove patch in the center of our sample area (Figures 5 and 6).

Figure 5. Location of mangrove to be removed.

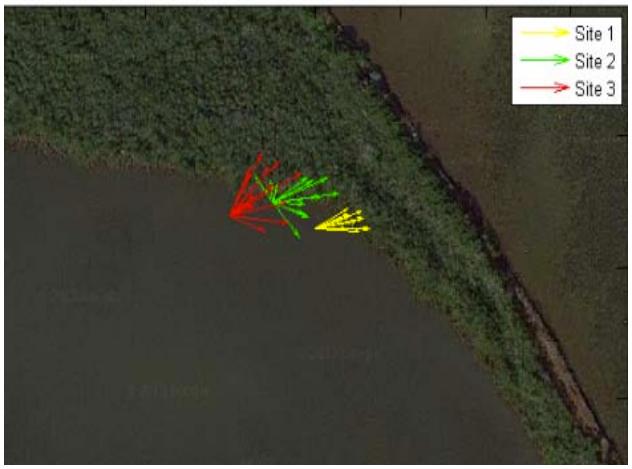

Figure 6. Current vectors measured on 9 June 2014.

Current measurements during the site survey showed that, in general, currents flow toward the northeast (Figure 6). Based on the survey results, the decision was made to deploy the instruments as close as possible to the mangroves. The current meter 2.5 m pond ward of the mangrove edge to avoid damage during mangrove removal (Figure 7). To capture effects of mangrove removal on circulation and benthic conditions, the position of the instrument package was located at the approximate mid-point, centered at 10.25 m, along the 20.5 m long stretch of mangroves to be removed (Figure 7). A second site survey measured the tidal range over one diurnal cycle from 5/16/2014 - 5/17/2014 by deploying a current meter at the chosen site (X) (Figure 7) over a period of 24 hours, to make sure the instrument package would not be exposed at low tide.

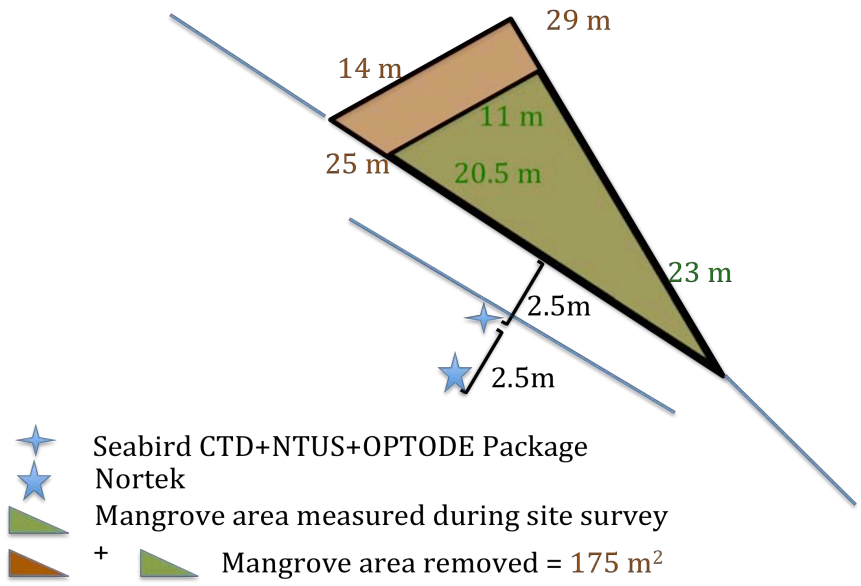

Figure 7. Site area and instrument package location. Schematic of the proposed coverage of mangrove to be removed (green shade) and actual area removed (green and brown shade). Instrument locations are marked: CTD (diamond) and current meter (star).

Mangrove removal

The workers and volunteers of the non-profit group Paepae o He'eia have been removing the invasive mangroves since 2006 as part of their fishpond restoration efforts. The mangroves are removed by topping the trees down to the sediment water interface during low tide, when the sediment is exposed. When the tide rises the salt water infiltrates and kills the roots and prevents regrowth. The remaining mangrove roots hold on to the sediment and it takes time for the sediment to be washed out of the area as the roots decompose.

The mangrove patch (Figure 3) was removed in three phases between June 17 and June 30, due to the timing of availability of the volunteer groups. On June 17, 99% of the trees were topped off and 50% of the roots were removed: an 87 m^2 area of roots above the sediment remained on the side adjacent to the site (Figure 8). On June 27 an additional 18% of roots above the sediment were removed (Figure 9). On June 30, 100% of mangrove roots above the sediment were successfully removed (Figure 10).

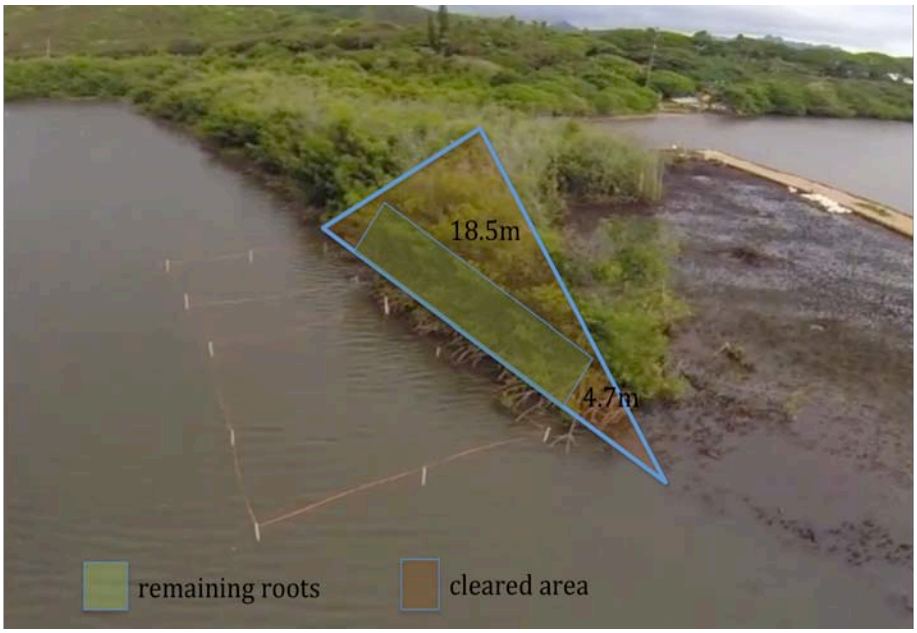

Figure 8. Aerial view of mangrove removal 1. Mangrove removal phase 1/3 on June 17, 2014, 99% of the mangrove trees topped off (brown shade) and 50% of roots above the sediment remaining (green shade).

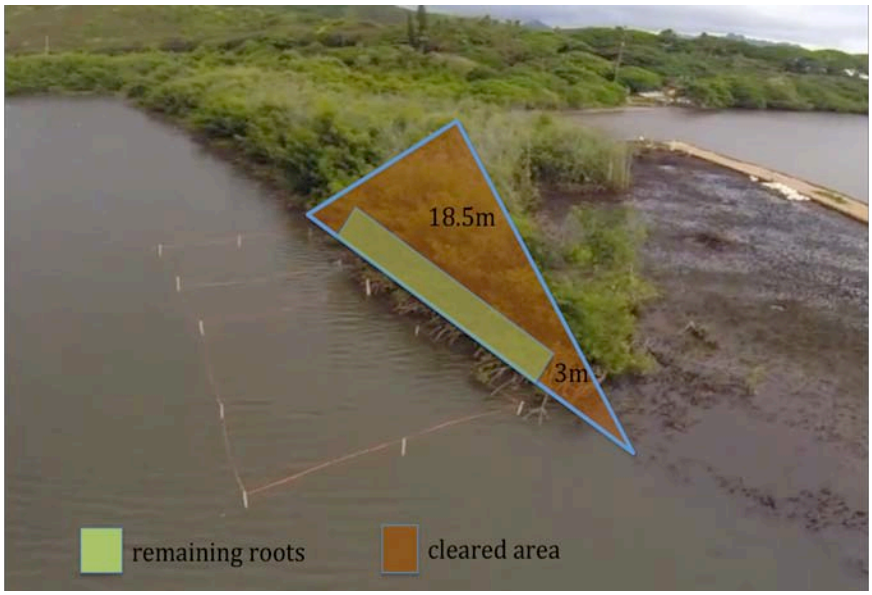

Figure 9. Aerial view of mangrove removal 2. Mangrove removal phase 2/3 on June 27, 2014, mangrove removed (brown shade) and mangrove 56% of mangrove roots above the sediment remaining (green shade).

Figure 10. Ground view of study site post-mangrove removal. Mangrove removal phase 3/3, 100% of mangroves removed on June 30, 2014.

Instrument Deployment

Instrumentation (please see following section on *in situ* instrumentation) was deployed at the sediment-water interface for a 68-day period between June 10 and August 15, 2014. *In situ* data was collected for a full spring to neap tidal cycle prior to mangrove removal, between June 10 and June 17. At the end of this pre-removal period instruments were taken out of the water to avoid damage during the major phases of mangrove removal, which started on June 17. On June 18 the instruments were re-deployed to monitor the effect of partial mangrove removal. On June 30 the instruments were taken out of the water a second time and re-deployed on the same day after mangrove removal was complete. The instruments were then left in place to monitor the conditions post-mangrove removal, which covered 7 spring to neap cycles between June 30 and August 15. Instruments were monitored and cleaned every 3 days throughout the study to avoid any sedimentation or biofouling.

In Situ Instrumentation

An instrument package was placed on the sea bed of the fishpond in the center of the study area adjacent to the mangrove patch. The location for the instrument package was determined during the initial site survey. The instrument package consisted of a Seabird Electronics 16plus CTD with a WET Labs Inc. ECO-NTUS transmissometer with biowiper™ (125 NTU range) and an Aanderaa oxygen sensor. The sampling interval was 4 minutes for the Seabird CTD and WETLabs ECO-NTUS. The instrument package was weighted to the bottom by a single chain link weighing ~90 lbs. at a distance 2.5 m away

from the edge of the mangrove patch. A Nortek current meter was deployed 2.5 m away from the CTD package, 5 m away from the mangrove patch, and had to be placed inside a 50 cm deep hole in the sediment to be kept in vertically place. Data from the current meter were continuously collected on a 4-minute interval.

Weather data

Wind data was obtained from NOAA's National Buoy Database Center (NBDC) online for Coconut Island: station mokh1 at Moku o Loe, HI located 21°25'59" N 157°47'23" W. Wind data from MCBH station was also obtained from Kāneʻohe Marine Corps air Station (KBMCB) from NOAA's National Weather Service online. Precipitation data for the Heʻeia watershed was obtained from NOAA's National Climate Data Center online for station KĀNEʻOHE 838.1, HI located 21°25'23" N, 157°48'04" W at elevation: 60'. Stream flow data for Heʻeia Stream was available through the USGS National Water Information System online for station 16275000 Heʻeia Stream at Haiku Valley in Kāneʻohe, HI. Storm data and maps were obtained from NOAA's Pacific Hurricane Center.

Data Processing

Data were processed and analyzed, and figures were made using Matlab R 2014. Spectral analyses were done on the time series data for pressure, currents, salinity, temperature and turbidity. Spectra were calculated by applying the Fourier transform to the data in Matlab.

CHAPTER III. RESULTS

Full Study

The data collected for He‘eia Fishpond June 10 to August 15, 2014, from *in situ* instrumentation (pressure, temperature, salinity, turbidity and current velocity) and from external environmental data (wind velocity, precipitation and stream discharge) are plotted as a time series in Figure 11. Data averages, minimum and maximum values for the full study are presented in Table 1.

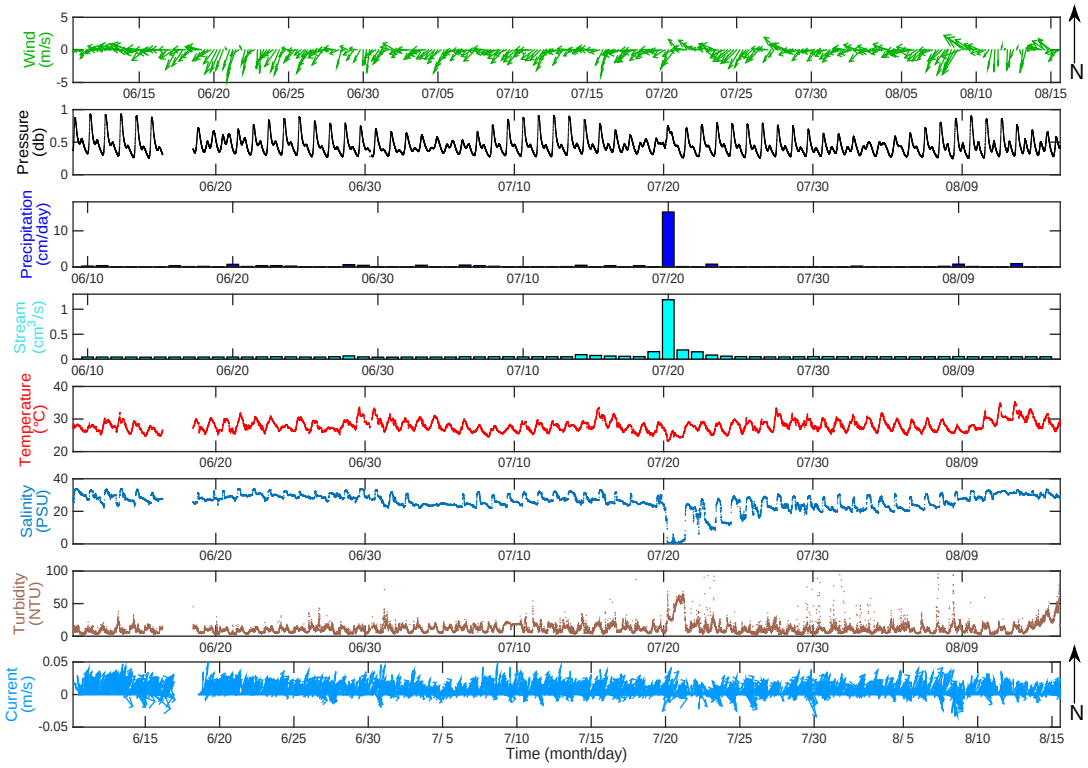

Figure 11. Time series of He‘eia Fishpond, June 10 – August 15, 2014. A) Wind velocity (m/s), B) Pressure (db), C) Precipitation (cm/d), D) Stream flow (cm^3/s), E) Temperature (°C), F) Salinity (PSU), G) Turbidity (NTU), H) Current Velocity (m/s).

Table 1. Full study He‘eia Fishpond, June 10 – August 15, 2014. Averages, minimum and maximum values for all data collected from 06/10/14 to 08/15/14 at study site in He‘eia Fishpond.

Table I. FULL STUDY 6/10/14-8/15/14				
	average	min	max	mode
WIND SPEED (m/s)	5.8	0	15.8	
WIND DIRECTION (°)				89
PRESSURE (db)	0.459	0.247	0.932	
PRECIPITATION (cm./day)	0.40	0	15.19	
STREAM DISCHARGE (m^3/s)	0.07	0.04	1.19	
SEA TEMPERATURE (°C)	27.942	23.307	35.300	
SALINITY (PSU)	25.946	0.363	33.855	
TURBIDITY (NTU)	12.08	1.94	99.96	
CURRENT SPEED (m/s)	0.062	0	0.263	
CURRENT DIRECTION (°)				90

For the duration of the study the wind was blowing predominantly from the northeast direction (trade winds) (Figure 11A), with the exception of episodic wind events, when the wind blew from the southeast for 2 to 3 days. The wind speed ranges from a minimum of 0 m/s to a maximum of 15.8 m/s (Table 1). The most common wind direction is 89° degrees with an average velocity of 5.8 m/s (Table 1).

The tide is a semidiurnal mixed tide with distinct spring and neap cycles (Figure 11B). The tidal range is between 0.247 db and 0.932 db, with an average pressure of 0.459 db (Table 1).

There is no rain on 18 out of 68 days, and the average precipitation is 0.40 cm (Table 1). There is a large precipitation event with 15.19 cm of rainfall over a 24-hour period (Figure 11C).

Stream discharge upstream, at He‘eia Stream, is on average 0.07 cm^3/s with a minimum discharge of 0.04 cm^3/s and a maximum discharge of 1.19 cm^3/s (Figure 11D, Table 1).

Temperature fluctuates daily with solar insolation. Temperature ranges between a minimum of 23.307 °C and maximum of 35.300 °C, averaging 27.942 °C (Figure 11E, Table 1).

The salinity fluctuates daily with the tides, and ranges from a minimum of 0.363 PSU to a maximum of 33.855 PSU with an average value of 25.946 PSU (Figure 11F, Table 1).

Turbidity fluctuates daily and shows an increasing trend starting half way through the study (Figure 11G). Fluctuations in turbidity vary between 1.94 NTU and 99.96 NTU with an average of 12.08 NTU (Table 1).

Current flow speeds range from a minimum of 0 m/s up to 0.263 m/s with an average flow speed of 0.062 m/s (Table 1). The most common current flow direction is 90°, towards the east (Table 1). The time series displays current magnitude vectors predominantly flowing towards the northeast (Figure 11H); it is difficult to discern currents flowing in an eastward direction on this type of plot.

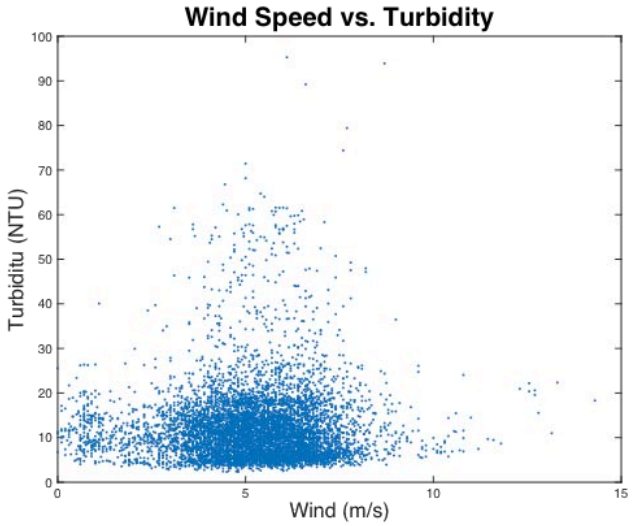

Figure 12. Plot of wind velocity vs. turbidity. Wind speed (m/s) on the x-axis versus turbidity (NTU) on the y-axis.

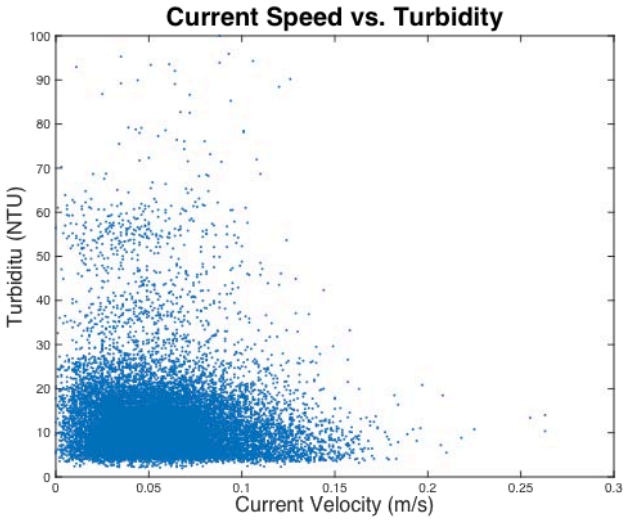

Figure 13. Plot of current velocity vs. turbidity. Current velocity (m/s) on the x-axis versus turbidity (NTU) on the y-axis.

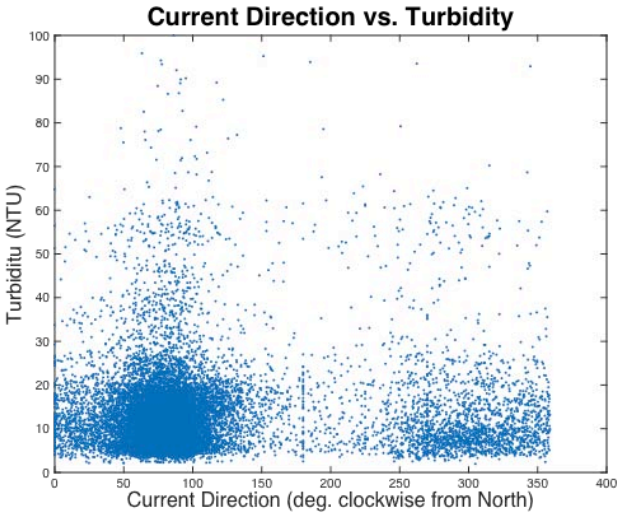

Figure 14. Plot of current direction vs. turbidity. Current direction (deg.) on the x-axis versus turbidity (NTU) on the y-axis.

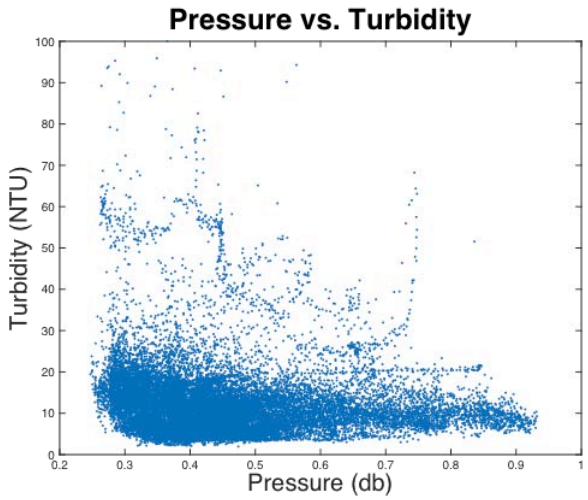

Figure 15. Plot of pressure vs. temperature. Pressure (db) on the x-axis versus temperature (°C) on the y-axis.

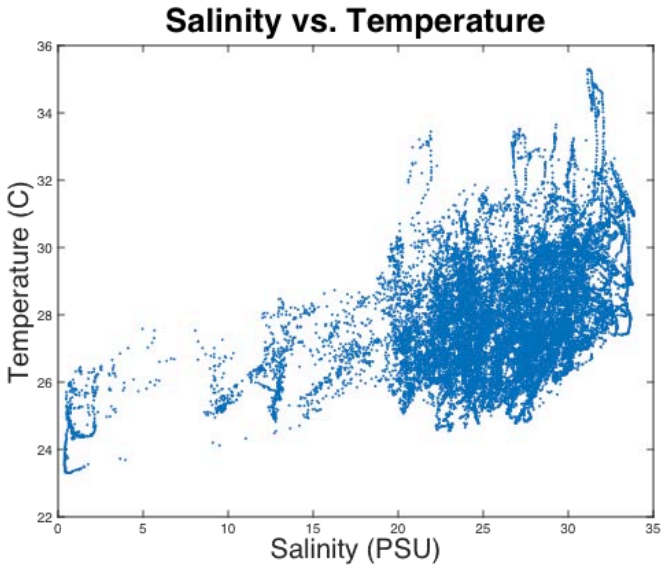

Figure 16. Plot of salinity vs. temperature. Salinity (PSU) on the x-axis versus temperature (°C) on the y-axis.

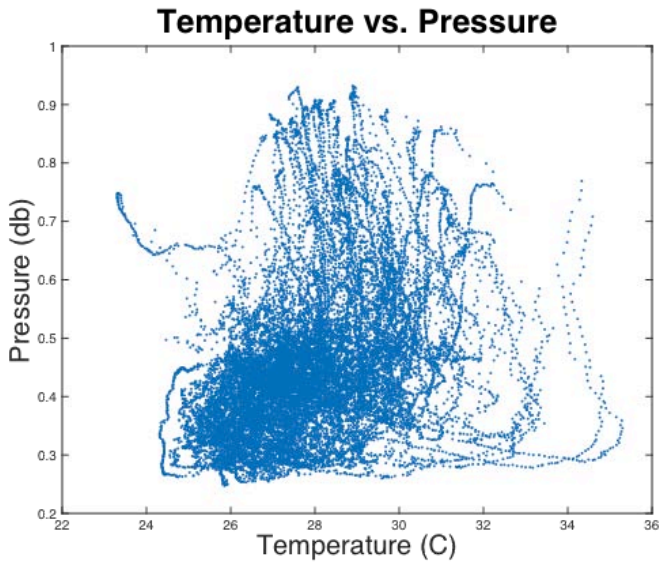

17. Plot of temperature vs. pressure. Temperature (°C) on the x- axis versus pressure (db.) on the y-axis.

Variations in Turbidity

Wind: Turbidity is highest when wind velocity is in the mid-range of speeds (~5 m/s) (Figure 12). Turbidity is highest at low current velocity (Figure 13).

Current Direction: The current directions are predominantly from 90° (E) (Table 1). Turbidity concentrations are highest when current flow is between 60° and 90° (E-NE) (Figure 14).

Tides: During low tides, turbidity is higher than at high tides (Figure 15).

Variations in Salinity and Temperature

Salinity and temperature are positively correlated with higher salinity occurring when temperatures are higher (Figure 16). Temperature is generally lower at low tide than at high tide (Figure 17).

Spectral Analysis

Dominant signals in the spectral analysis for pressure are the lunar diurnal constituent frequency (K1 = 0.98 d^{-1}) and the principal lunar semidiurnal frequency (M2 = 0.52 d^{-1}) (Figure 18), these correspond to periods of 24.59 hr. and 12.16 hr., respectively (Figure 19). The dominant frequency signals of the currents are K1 = 0.98 d^{-1} and M2 = 0.52 d^{-1}. (Figure 20). Temperature fluctuations occur at periods of 23.05 hr. and 11.89 hr. (Figure 21). Salinity fluctuates at the main periods of 24.59 hr. and 12.16 hr. (Figure 22). Turbidity periodically peaks every 25.15 hr. and 12.26 hr. (Figure 23).

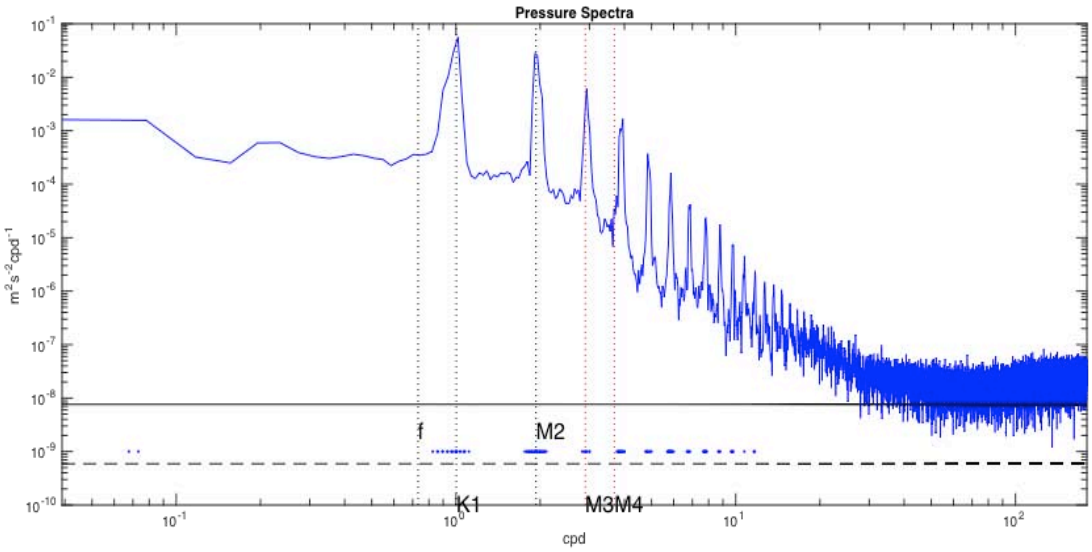

Figure 18. Spectral analysis of pressure. From June 30 –August 15, 2014, with cycles per day on the x-axis and energy ($m^2s^{-2}cdp^{-1}$) on the y-axis. The main tidal harmonic signals are marked f, K1, M2, M3, M4.

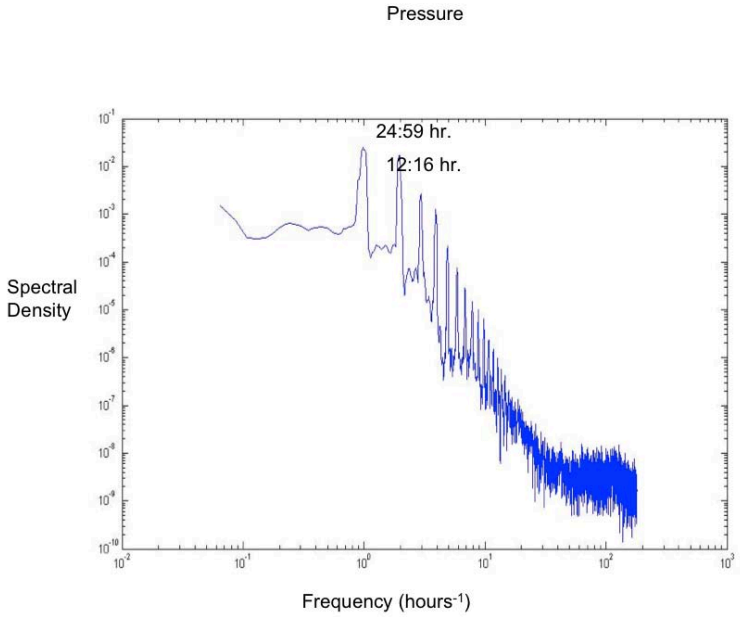

Figure 19. Spectral analysis of Pressure (2). From June 30 – August 15, 2014, with frequency ($hours^{-1}$) on the x-axis and spectral density on the y-axis. The two main harmonic peaks are marked in hours.

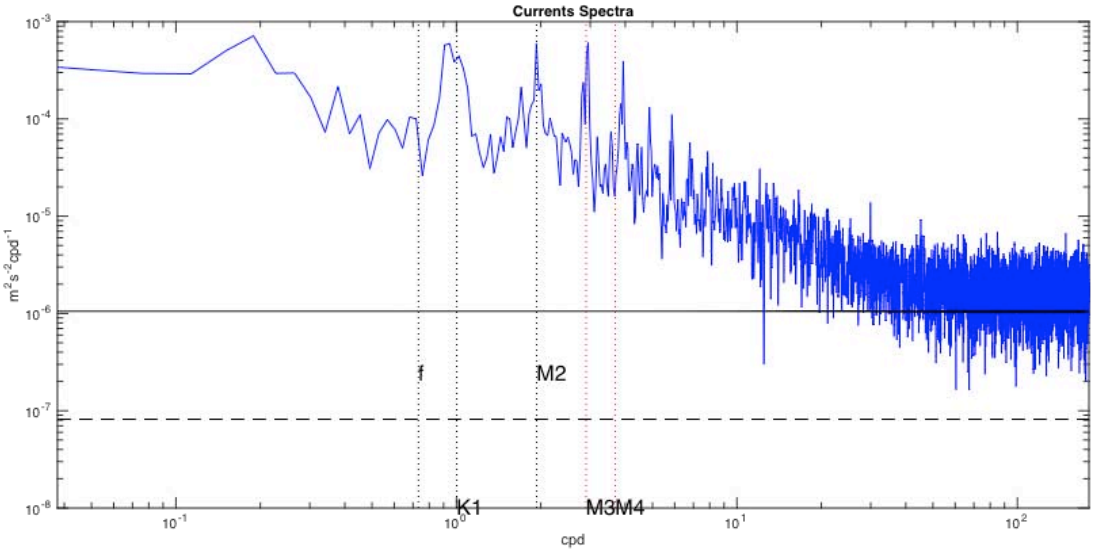

Figure 20. Spectral analysis of currents. From June 30 – August 15, 2014, with cycles per day on the x-axis and energy ($m^2s^{-2}cdp^{-1}$) on the y-axis. The main tidal harmonic signals are marked f, K1, M2, M3, M4.

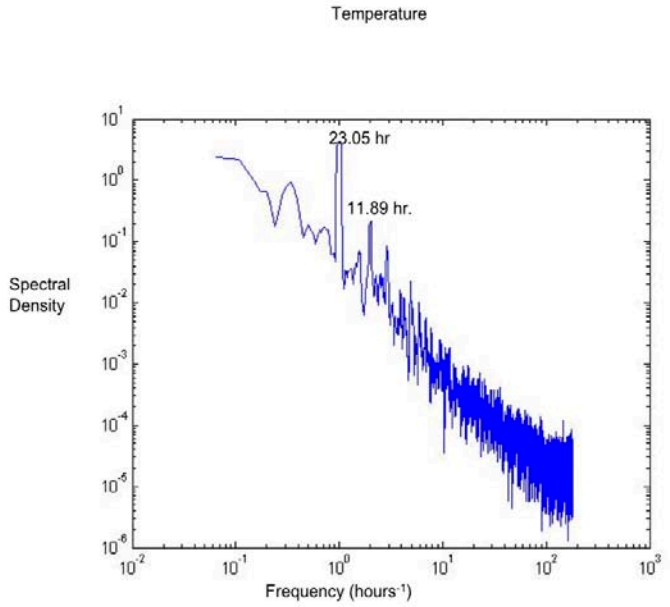

Figure 21. Spectral analysis of Temperature. From June 30 – August 15, 2014, with frequency ($hours^{-1}$) on the x-axis and spectral density on the y-axis. The two main harmonic peaks are marked in hours.

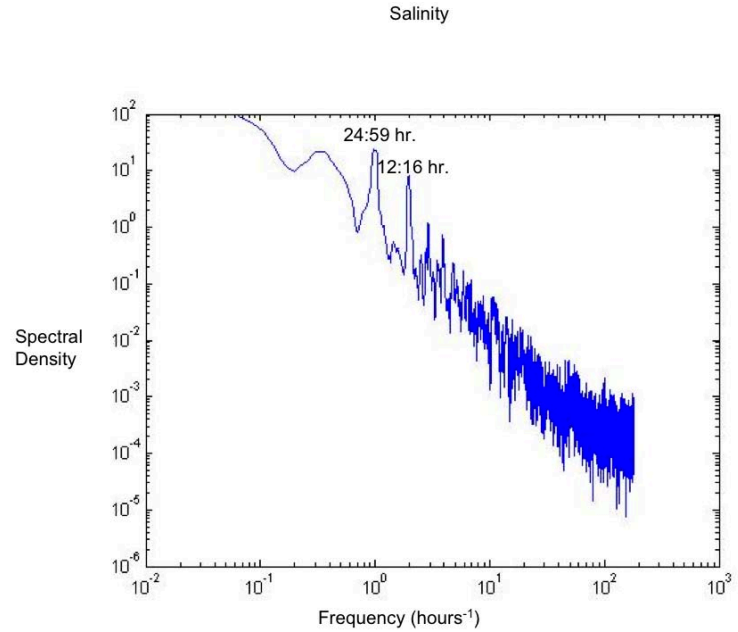

Figure 22. Spectral analysis of Salinity. From June 30 – August 15, 2014, with frequency (hours^{-1}) on the x-axis and spectral density on the y-axis. The two main harmonic peaks are marked in hours.

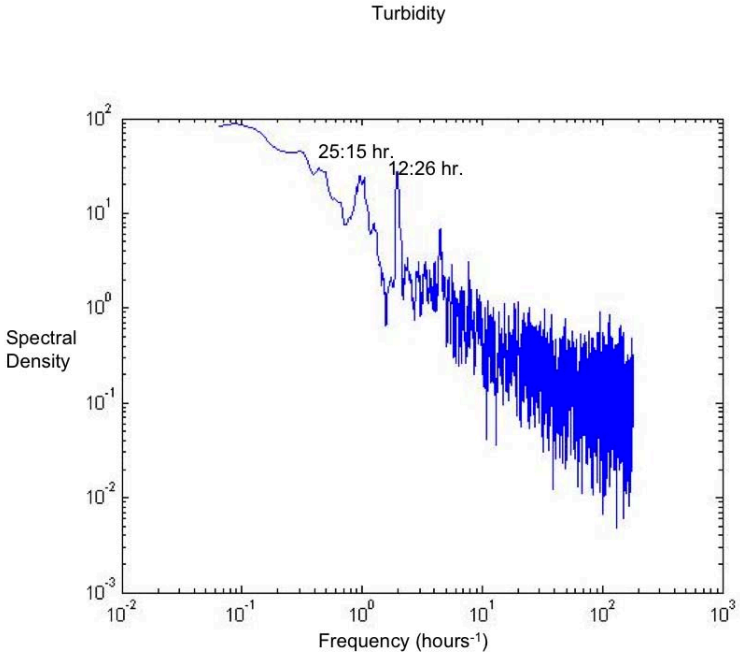

Figure 23. Spectral analysis of Turbidity. From June 30 – August 15, 2014, with frequency (hours^{-1}) on the x-axis and spectral density on the y-axis. The two main harmonic peaks are marked in hours.

The Daily Tidal Cycle

A finer scale of resolution is required to see changes in current flow with the daily ebb and flood of the tides (Figure 24). The currents flow toward the northeast during ebb and flood tides but flow toward the south during slack tide (Figure 24).

The fluctuations of temperature, salinity and turbidity are correlated with the tidal stage (Figure 24). Salinity is higher at high tide than at low tide. Temperature also increases at high tide (Figure 24). Turbidity follows the opposite trend with higher concentrations at low tide rather than high tide (Figure 24).

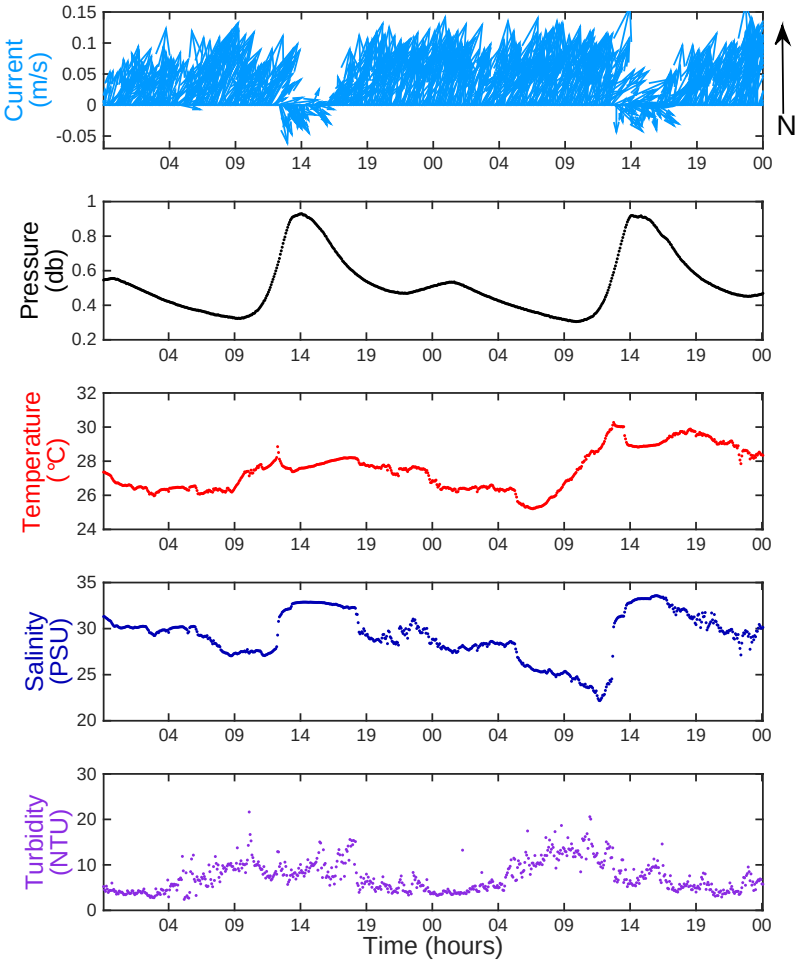

Figure 24: Time series of He‘eia Fishpond over a tidal cycle (48 hours), June 11 – June 12, 2014. A) Current Velocity (m/s), B) Pressure (db), C) Temperature (°C), D) Salinity (PSU), E) Turbidity (NTU).

Table 2. Baseline, Pre-Mangrove Removal He‘eia Fishpond June 10 – June 17, 2014. Average, minimum and maximum values for physical parameters at study site in He‘eia Fishpond before mangrove removal.

Table 2. Baseline: PRE-REMOVAL: 6/10/14-6/17/14				
	average	min	max	mode
WIND SPEED (m/s)	5.8	0.3	10.0	
WIND DIRECTION (°)	90	0	360	90
PRESSURE (db)	0.503	0.255	0.932	
PRECIPITATION (cm./day)	0.14	0	0.38	
STREAM DISCHARGE (m^3/s)	0.04	0.04	0.05	
SEA TEMPERATURE (°C)	27.338	24.776	31.952	
SALINITY (PSU)	28.692	22.181	33.761	
TURBIDITY (NTU)	8.90	2.41	37.53	
CURRENT SPEED (m/s)	0.081	0.002	0.220	
CURRENT DIRECTION (°)	90			90

Pre-Removal / Baseline

To determine whether certain events had any impacts on the physical conditions in He‘eia Fishpond, average baseline conditions were calculated for the monitoring period pre-mangrove removal.

Baseline conditions were calculated based upon data taken during a spring to neap tidal cycle from June 10 to June 17, 2014: this period was pre-mangrove removal. Wind speeds are on average 5.8 m/s blowing from the east-northeast, while currents have average speeds of 0.081 m/s and flow towards the northeast (Table 2). Average precipitation is 0.14 cm/day while stream discharge is 0.04 cm^3/s (Table 2). Mean temperature is 27.338 °C, salinity mean is 28.692 PSU and turbidity mean is 8.90 NTU (Table 2).

Post-Removal

There are interesting differences in physical attributes of the pond when one compares pre-mangrove (baseline) and post-mangrove removal periods. Wind speed does not exhibit significant changes between the two periods; there is only a 5% decrease in wind speed from the pre-removal to the post-removal phase. Precipitation, however, is 32% higher during the post-mangrove removal period. Following an increase in precipitation, the average stream discharge also increases in the post-mangrove removal period by 30%. Changes in current speed are also

significant, however unlike precipitation and stream discharge, which increase during the post-removal period, current speed decreases by 24% during this period. Temperature and salinity experience a 10% and 9% decrease in the post-removal period, respectively. Turbidity displays a significant increase of 39% in the post-removal period. Likely the increase in turbidity seen in the post-removal phase is influenced by precipitation and stream discharge, as well as by the mangrove removal itself (Table 3).

Table 3. Post-Mangrove Removal He‘eia Fishpond June 30 – July 19, 2014. Average, minimum (min), maximum (max) values and deviation from baseline (deviation) for physical parameters at study site in He‘eia Fishpond during post-mangrove removal.

Table 3. POST-REMOVAL: 6/30/14-7/19/14						
	average	min	max	mode	deviation	%change
WIND SPEED (m/s)	5.5	0.6	11		-0.3	-5%
WIND DIRECTION (°)		14	246	88	-2	-2%
PRESSURE (db)	0.455	0.277	0.908		-0.048	-10%
PRECIPITATION (cm./day)	0.18	0	0.53		0.04	32%
STREAM DISCHARGE (m^3/s)	0.06	0.04	0.15		0.01	30%
SEA TEMPERATURE (°C)	24.554	33.522	27.759		-2.783	-10%
SALINITY (PSU)	26.195	21.546	33.179		-2.498	-9%
TURBIDITY (NTU)	12.33	3.14	86.79		3.43	39%
CURRENT SPEED (m/s)	0.062	0	0.195		-0.020	-24%
CURRENT DIRECTION (°)				90	0	0%

Storms

In the summer of 2014, tropical cyclones affected the physical characteristics of He‘eia Fishpond. Data averages, minimum and maximum values are summarized in Tables 4, 5 and 6 and compared with baseline pre-removal data in Table 1.

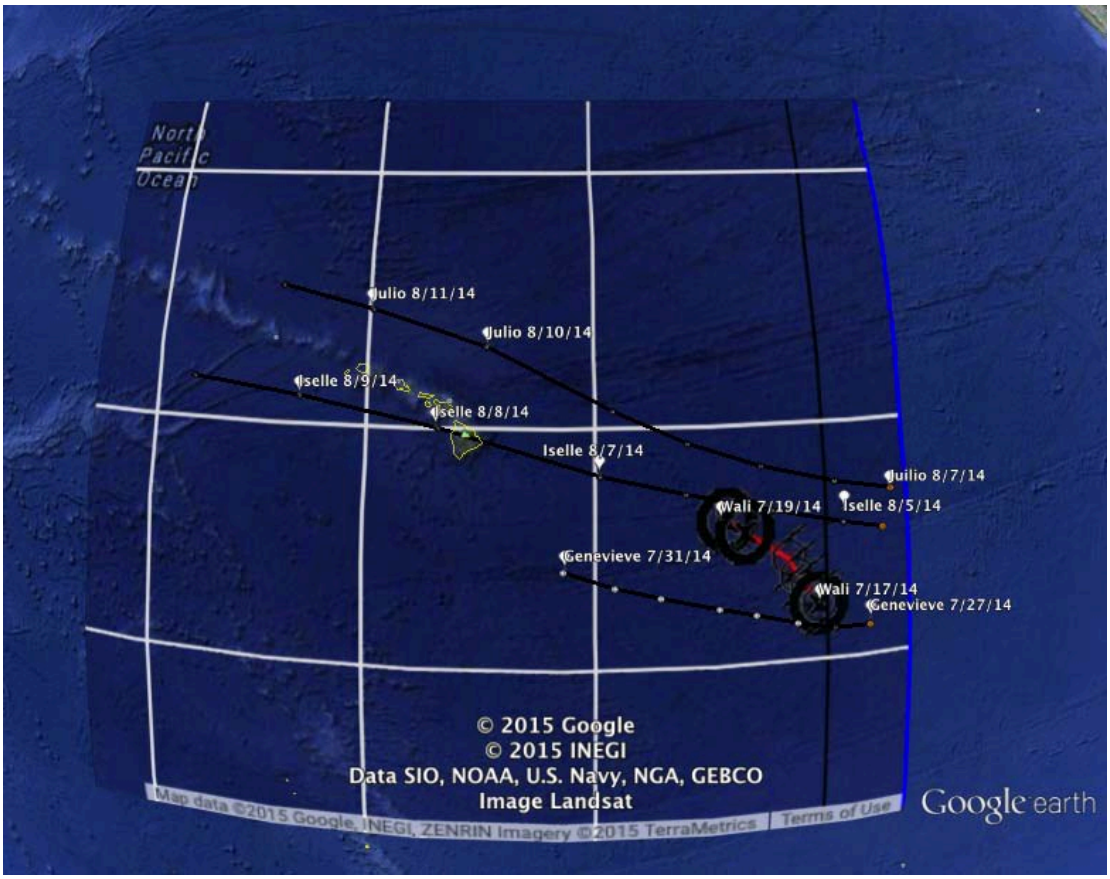

Figure 25. Map of tropical storm tracks in the North Pacific Ocean during the study period, June 10 – August 15, 2014. Wali: 7/17/14 - 7/27/14, Genevieve: 7/27/14 - 7/31/14, Iselle: 8/5/14 - 8/10/14 and Julio: 8/7/14 - 8/11/14. (Google Earth, NOAA, 2015)

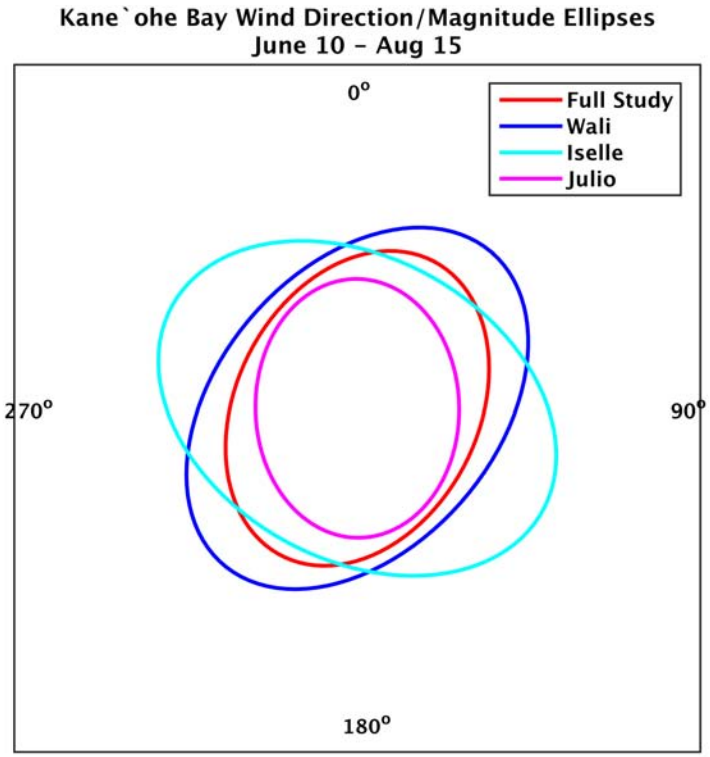

Figure 26: Plot of magnitude and direction for winds in Kāneʻohe Bay. Data from KBMCB, for the full study (red) and during tropical storms, Wali (blue), Iselle (cyan), Julio (magenta), the y-axis is North.

Tropical Storm Wali

The first tropical storm of the 2014 north Pacific hurricane season formed on July 17 in the North Eastern tropical Pacific Ocean. On July 17, tropical storm Wali's center was located 1070 mi. southeast of Hilo, near 12.7° N 140.7° W (NOAA, 2014). By July 19 the storm was downgraded to a tropical depression located near 12.8° N 140.8° W. The depression degraded into a post-cyclone after July 19 and brought heavy rain to the Hawaiian Islands on July 20 (Table 4.1). Heʻeia watershed was affected by storm conditions and flash flood warnings on July 20 and received a total rainfall of 15.19 cm. (Table 4.1). Heʻeia Stream discharge increased by >2500% relative to baseline flow and remained above average for the duration of the study (Table 4.2). Winds shifted from the southeast and weakened by 7% (Table 4.1). The predominant currents shifted by 90°, towards the north during tropical storm Wali, and displayed the strongest pulses of velocity of the study period, although the average values for the storm are 24% lower than during baseline conditions (Table 4.1). Tropical storm Wali also affected the water level in the fishpond. During low tide, water levels do not drop to "normal" levels; on average the water level at the study site is 9% higher during Wali than during baseline conditions (Table 4.1). During Wali, the average salinity is reduced by 81% and average temperatures are reduced by 8% (Table 4.1). Accompanying significant increases in water level, precipitation, and stream discharge, the average turbidity increased by 257% during Wali (Table 4.1).

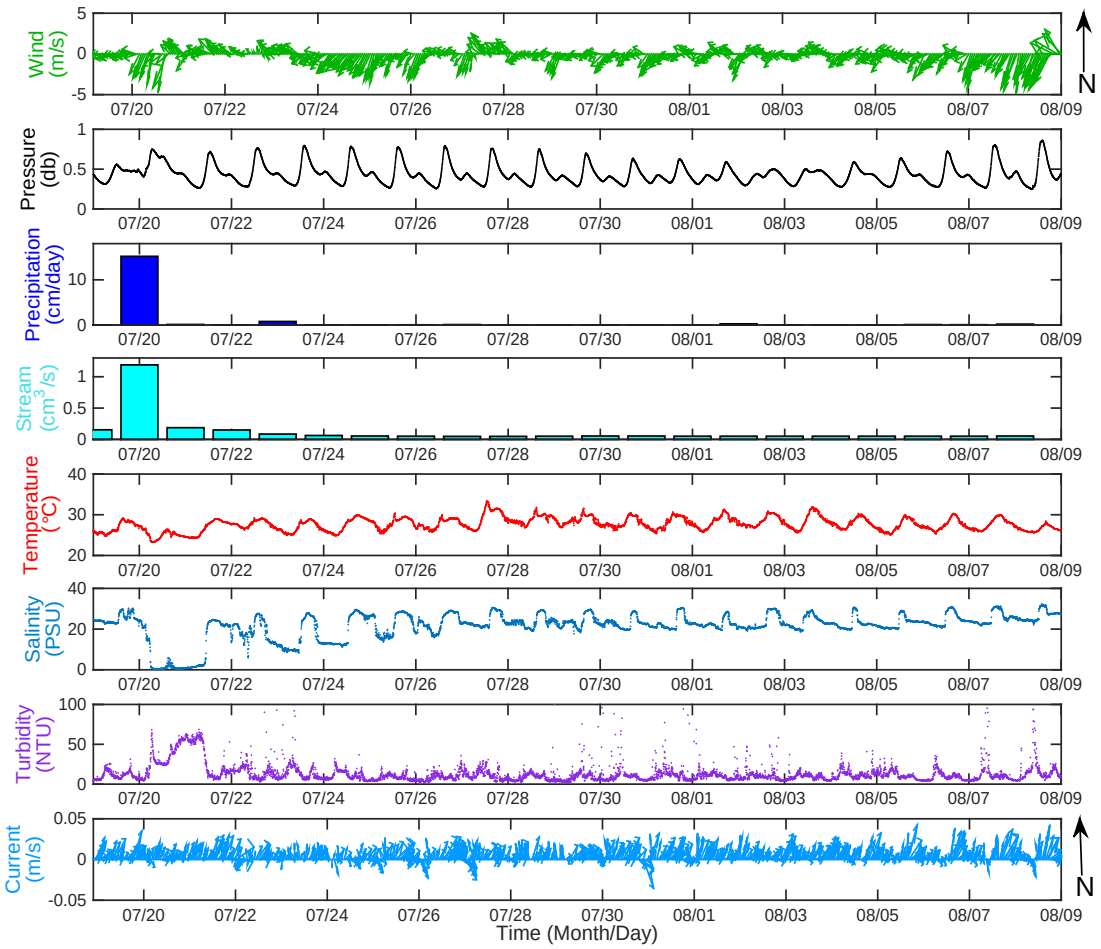

Figure 27. Time series for He‘eia Fishpond: effects of tropical storm Wali, July 19 – August 9, 2014. A. Wind velocity (m/s), B. Pressure (db), C. Precipitation (cm/d), D. Stream flow (cm^3/s), E. Temperature (°C), F. Salinity (PSU), G. Turbidity (NTU), H. Current Velocity (m/s).

4.1. Tropical Storm Wali: He‘eia Fishpond July 20, 2014. Average, minimum (min), maximum (max) values, deviation from baseline (deviation), percent change (% change), and recovery rate, in days, for physical parameters at study site in He‘eia Fishpond during tropical storm Wali on 07/20/14.

Table 4.1. Tropical Storm WALI: 7/20/14						
	average	min	max	mode	deviation	%change
WIND SPEED (m/s)	5.3	0.3	10.8		-0.4	-7
WIND DIRECTION (°)	100	1	353	100		
PRESSURE (db)	0.548	0.404	0.748		0.045	9
PRECIPITATION (cm./day)	15.18				15.05	10915
STREAM DISCHARGE (m^3/s)	1.19				1.14	2549
SEA TEMPERATURE (°C)	25.128	23.307	27.326		-2.210	-8
SALINITY (PSU)	5.456	0.363	24.550		-23.236	-81
TURBIDITY (NTU)	31.75	4.33	68.25		22.86	257
CURRENT SPEED (m/s)	0.062	0	0.263		-0.019	-24
CURRENT DIRECTION (°)	0			0		

	Recovery Rate (days)
WIND SPEED (m/s)	3
WIND DIRECTION (^{0})	3
PRESSURE (db)	1
PRECIPITATION (cm./day)	1
STREAM DISCHARGE (m^3/s)	19
SEA TEMPERATURE (^{0}C)	7
SALINITY (PSU)	19
TURBIDITY (NTU)	no recovery(>25)
CURRENT SPEED (m/s)	1
CURRENT DIRECTION (^{o})	1

Post Tropical Storm Wali

Precipitation returned to baseline levels the day after Wali passed (Table 4.1). However, stream discharge remained above baseline conditions for 19 days. Winds returned to normal within 3 days (Table 4.2). Sea temperature recovered after 7 days and the average salinity recovered to baseline conditions after 19 days (Table 4.2). Turbidity levels remained elevated for the duration of the study (25 days) and did not recover to baseline conditions (Table 4.2).

Table 4.2. Post Tropical Storm Wali HFP July 21 – August 8, 2014. Average, minimum (min), maximum (max) values and deviation from baseline (dev.) for physical parameters at study site in He‘eia Fishpond post tropical storm Wali on 07/21/14 – 8/15/14.

Table 4.2. POST-WALI RECOVERY RATES: 7/21/14 - 8/15/14

	21-Jul		27-Jul		9-Aug		15-Aug	
	average	dev.	average	dev.	average	dev.	average	dev.
WIND SPEED (m/s)	5.5	-0.3						
WIND DIRECTION (^{0})	92	2		-90				
PRESSURE (db)	0.440	-0.067		-0.503				
PRECIPITATION (cm./day)	0.13	-0.01		-0.14				
STREAM DISCHARGE (m^3/s)	0.19	0.14	0.05	0.003	0.05	0.01		
SEA TEMPERATURE (^{0}C)	26.78	-0.560	27.678	0.341				
SALINITY (PSU)	13.256	-15.437	19.630	-9.062	28.834	0.1412		
TURBIDITY (NTU)	31.78	22.88	14.90	6.01			14.1932	5.3023
CURRENT SPEED (m/s)	0.062	-0.019	0.047	-0.034				
CURRENT DIRECTION (^{o})	90	0	90	0				

Tropical Storms Iselle and Julio

On August 1 2014 Hurricane Iselle started developing an eye 1730 mi. southeast of the island of Hawai‘i and developed into a category 4 hurricane on August 4 (NOAA, 2014). Due to dry air conditions the cyclone weakened into a category 1 hurricane on August 6. Hurricane Iselle made landfall on eastern Hawai‘i at 12:30 am on August 8 2014 (NOAA, 2014). The high elevation mountains of Hawai‘i disrupted the cyclonic circulation of Iselle (NOAA, 2014). On August 8 at

5 am tropical storm Iselle was located 290 km west southwest of Oahu (Honolulu, Hi), with maximum sustained winds of 85 km/h, by 11 am the storm was located 200 km south of Oahu and by 2 pm it was 195 km southwest of Oahu with maximum sustained winds of 65 mph (NOAA, 2014).

Iselle affected He‘eia with sustained winds above 15.8 m/s, a 175% increase in average wind speeds (Figure 25), and 0.20 cm of precipitation on August 8 (Table 5). At the same time salinity recovered to baseline levels following the perturbation from prior tropical storm Wali (Table 5). Behind tropical storm Iselle, followed tropical storm Julio passing north of the Hawaiian Islands, 630 km north east of Honolulu at 11:00 am on 8/10/14 causing no direct impacts to the Hawaiian Islands (NOAA, 2014). On August 11 and 12, following the double storms Iselle and Julio, the average winds weakened by 177% and shifted from the north (Table 6.1). Temperature increased by 12% and peaked at 35.300 ^{o}C on August 12. Salinity average increased by 9% (Table 6.2).

Table 5. Tropical Storm Iselle He‘eia Fishpond August 8, 2014. Average, minimum (min), maximum (max) values, deviation from baseline (deviation) and percent change (% change) for physical parameters at study site in He‘eia Fishpond during tropical storm Iselle 08/08/14.

Table 5. Tropical Storm ISELLE: 8/8/14						
	average	min	max	mode	deviation	%change
WIND SPEED (m/s)	15.8	3.4			10.0	174
WIND DIRECTION (°)		9	148	65	-25	
PRESSURE (db)	0.456	0.247	0.858		-0.092	-9
PRECIPITATION (cm./day)	0.20				0.07	47
STREAM DISCHARGE (m^3/s)	0.05	*Boarded	mākāhā		0.01	20
SEA TEMPERATURE (°C)	26.545	25.592	28.437		-0.793	-3
SALINITY (PSU)	26.587	22.048	32.206		-2.106	-7
TURBIDITY (NTU)	15.643	3.957	93.923		6.752	76
CURRENT SPEED (m/s)	0.059	0	0.179		-0.023	-28
CURRENT DIRECTION (°)				90	0	

Table 6.1. Tropical Storm Julio He‘eia Fishpond August 10, 2014. Average, minimum (min), maximum (max) values, deviation from baseline (deviation) and percent change (% change), for physical parameters at study site in He‘eia Fishpond during Hurricane Julio on 08/10/14.

Table 6.1. Hurricane JULIO: 8/10/14						
	average	min	max	mode	deviation	%change
WIND SPEED (m/s)	4.2	1.4	7.1		-1.6	-27
WIND DIRECTION (°)		6	106	87	-3	
PRESSURE (db)	0.464	0.260	0.859		-0.084	-8
PRECIPITATION (cm./day)	0.15				0.01	11
STREAM DISCHARGE (m^3/s)	0.05	*Boarded	mākāhā		0.01	14
SEA TEMPERATURE (°C)	29.029	26.734	32.544		1.692	6
SALINITY (PSU)	29.817	26.222	32.855		1.124	4
TURBIDITY (NTU)	10.34	2.74	59.41		1.45	16
CURRENT SPEED (m/s)	0.046	0	0.165		-0.035	-43
CURRENT DIRECTION (°)				90	0	

Table 6.2. Post Tropical Storm Julio Heʻeia Fishpond August 11 – 14, 2014 Average, minimum (min), maximum (max) values, deviation from baseline (deviation) and percent change (% change) for physical parameters at study site in Heʻeia Fishpond post Hurricane Julio heat event.

Table 6.2. POST-JULIO: 8/11/14-8/14/14						
	average	min	max	mode	deviation	%change
WIND SPEED (m/s)	2.1	0	4.8		-3.7	-64
WIND DIRECTION (°)	5	0	360	5	-85	
PRESSURE (db)	0.468	0.278	0.862		-0.035	-7
PRECIPITATION (cm./day)	0				-0.14	-100
STREAM DISCHARGE (m^3/s)	0.05	*boarded	mākāhā		0.01	14
SEA TEMPERATURE (°C)	31.026	27.874	35.300		3.688	13
SALINITY (PSU)	31.418	27.290	33.086		2.725	9
TURBIDITY (NTU)	9.54	1.94	26.27		0.65	7
CURRENT SPEED (m/s)	0.046	0.002	0.157		-0.035	-43
CURRENT DIRECTION (°)				90	0	

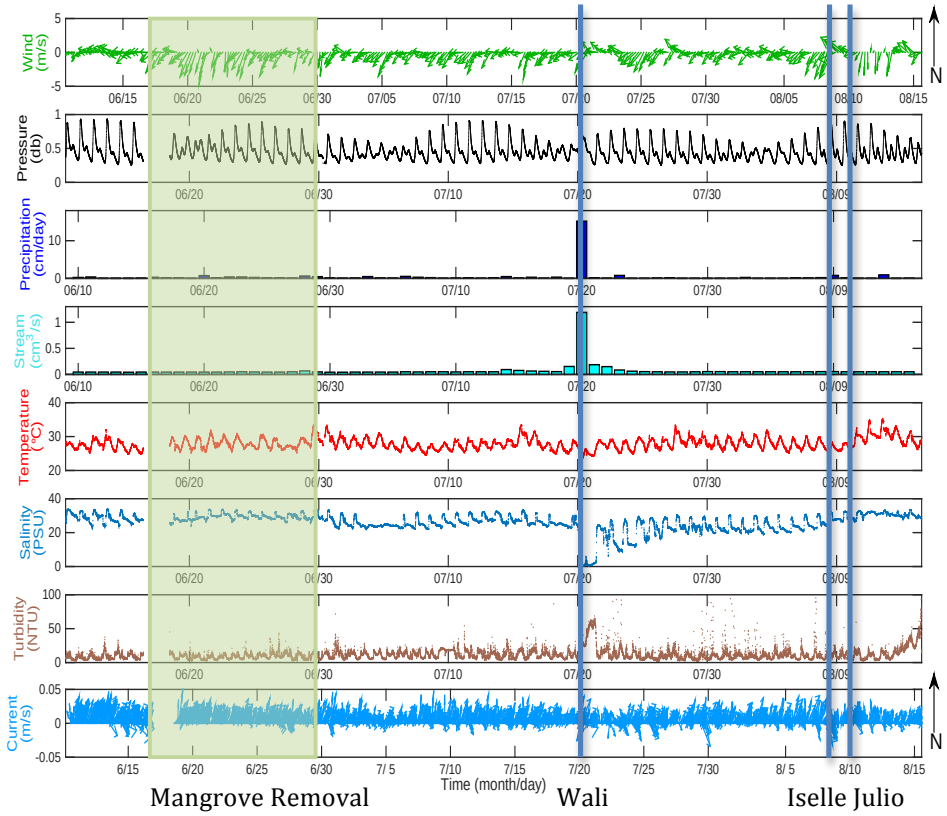

Figure 28. Main events during study and time series of He‘eia Fishpond, June 10 – August 15, 2014. Wind velocity (m/s), Pressure (db), Precipitation (cm/d), Stream flow (cm^3/s), Temperature (°C), Salinity (PSU), Turbidity (NTU), Current Velocity (m/s) from He‘eia Fishpond, June 10 – August 15, 2014, with main events highlighted: Mangrove removal (shaded in green), and tropical storms Wali, Iselle, Julio (blue lines).

He‘eia Fishpond is an ideal estuarine environment for investigating land-sea interactions between the He‘eia watershed and the Malauka‘a fringing reef of Kāne‘ohe Bay. The water flow in HFP is driven by physical forces. The water is bounded by the physical constraints of the semi-permeable rock wall on the ocean side of the fishpond, and the invasive mangrove forest on its land side. Environmental conditions in HFP are influenced by tides, wind, precipitation and stream discharge, which affect circulation, temperature, salinity and turbidity. The study site is representative of the estuarine conditions within HFP. Conditions affecting estuarine circulation such as tides and winds can be studied in this representative area. The scales of variability in the physical environment between June 10 and August 15, 2014 can be separated under five distinct conditions i) Pre-mangrove removal, ii) Post-mangrove removal, iii) A tropical storm with heavy

rains, iv) A tropical storm with high winds, v) A tropical storm during which time the HFP was managed (Figure 29).

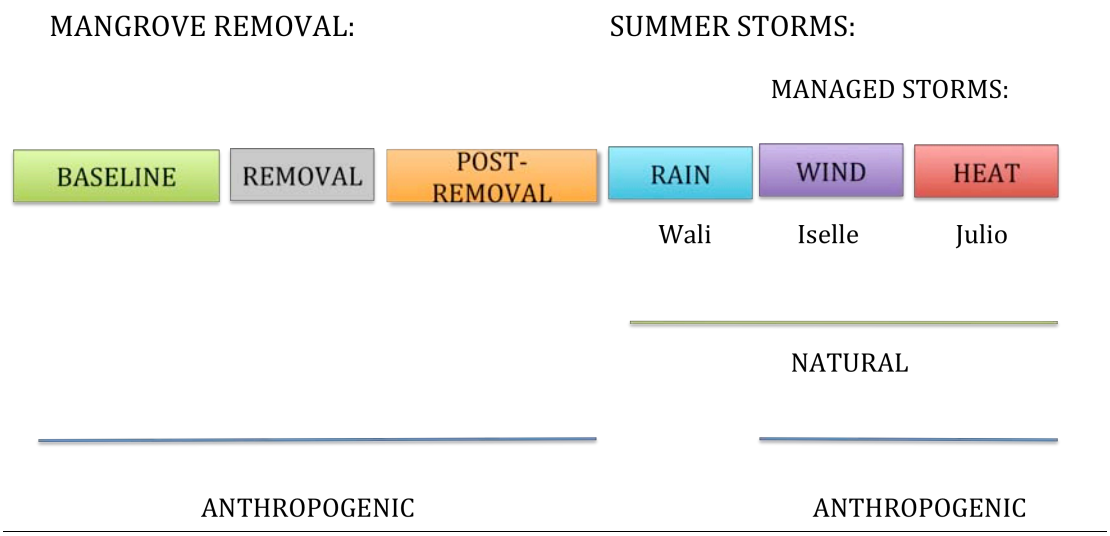

Figure 29. Main events during the study at He‘eia Fishpond. Sequence of events during the study and the main causes: natural and anthropogenic.

Baseline conditions

Conditions pre-mangrove removal are not influenced by natural or anthropogenic perturbation. Average conditions pre-removal are considered as baseline and provide a basis for comparison with changes in conditions for various events during the study. The physical characteristics of HFP that define its function as a semi-enclosed embayment have implications for tidal and current flow patterns. The currents at the study site are influenced by the diurnal tidal signal from the recirculation of water in and out of the pond wall mākāhā. The patterns of ebb and flow thorough the mākāhā occur at different rates, with flow discharge occurring more rapidly than ebb (D’Andrea, 2015). The pattern can be observed from spectral analysis, and the same trend is displayed for pressure and current velocity. The pond fills in rapidly during flow tide, the process is likely to be accelerated due to a break in the pond wall (OB). While the ebb tide is relatively slower because of the flow being restricted through the mākāhā. Thus, the main signal detected up by the currents is the northeast flow of the ebbing tide.

The predominant wind direction is from the east-northeast, which is the direction of the trade winds. The current flow at the site has a predominant direction toward the east-northeast. Thus, the current flow opposes the wind direction. I hypothesize this happens because fresh water from the river entering the fishpond creates a water surface that is a few centimeters higher near the river source. The increased height creates a pressure gradient that forces current flow against the wind direction. Thus the dominant forcing function on currents, for most of the time of the study, was the pressure gradient established by freshwater inflow.

The dominant tidal constituents are lunar diurnal (K1) and principal lunar semidiurnal (M2). Tides and currents fluctuate at the same frequency, with peaks at equal periods. Therefore tidal forcing is likely a significant driver of currents in HFP. Pressure and salinity maxima occur at exactly the same frequency, suggesting tidal forcing is critical for these properties. Turbidity frequency slightly lags (~15 minutes) pressure and currents, likely because some particles remain suspended and take some time to settle. Temperature peaks occur at a diurnal frequency in response to daily solar warming.

The turbidity is highest when the current direction is from the northeast, which is the same as the direction of wind flow. Diel tidal variations also affect turbidity levels, with lower water levels experiencing higher turbidity concentrations (Figure 17).

Salinity also fluctuates daily as a function of pressure. Salinity perturbations are result from seawater being diluted by the freshwater discharged from He‘eia Stream during intense precipitation events. Salinity fluctuations indicate which body of water has a predominant influence on pond water composition. Stream discharge lowers the salinity by dilution of the seawater with fresh water.

Winds for the study period were shifted 20 degrees towards the east compared to the average wind direction for November 2004 - November 2014 as calculated by McCoy et al. (*in prep.*). The shift in wind direction may be attributed to temperature anomalies in the Pacific that caused a decrease in the pressure gradient that drives the trade winds (Timmermann pers. comm.).

In the He‘eia region precipitation can be “flashy”, meaning that it can be episodic and short-lived, with an immediate response time for stream discharge (Hoover and Mackenzie 2009). The effect of flashy precipitation can be observed during tropical storm Wali on July 20. The persistence of the freshwater plume may be attributed to physical forcing controlled by stream discharge (Ostrander et al. 2007). When stream discharge is high following storm conditions, the pressure gradient from the estuarine flow can completely overcome the tidal signal, as seen during tropical storm Wali. Stream discharge is the main source of terrigenous input to the fishpond. High turbidity values occur during the period of time with the highest stream discharge values following the storm event.

Mangrove Removal

The effects of mangrove removal can be quantified by direct comparison of post-removal to pre-removal baseline values. Wind speeds are similar pre-removal and post-removal but the direction shifts from the northeast post-removal. No effects from mangrove removal can be observed on wind forcing at the study site due to the data coming from an external site in Kāne‘ohe Bay. The reduction of current speed post-removal may be due to the overall change in wind speed at the study site, the tidal phase, or due to the removal of the mangrove canopy, which acts as a windbreak. The removal of the mangrove canopy could increase the wind forcing on the specific study area, thus decrease the current speed, because the two are in opposition. The mangrove removal process released fine-grained sediment causing an increase in the turbidity levels of the water by 39% relative to pre-mangrove removal values. The increase in turbidity may also have

been due to increases in precipitation and stream discharge, however (Table 3). The slight decrease in temperature and salinity post-removal may be due to the increase in fresh water from increased stream discharge.

Storms

The summer of 2014 was characterized by an unusually high frequency of tropical storms attributed to mild El Niño conditions in the southeastern Pacific Ocean. Ocean temperatures were up to 2 degrees higher in 2014 (Timmerman pers. comm.). Warmer ocean waters can lead increased to storm activity. An El Niño watch was issued during the study period with a 65% - 70% chance of an El Niño developing in the Northern Hemisphere winter during the months of June to August 2014 (NOAA, 2014). Sea surface temperature anomalies were above the heat anomaly threshold of +0.5 °C during the summer of 2014 (NOAA, 2014). El Niño is a driver for hurricanes in the Pacific, it increases the frequency of tropical cyclones in the area due to warmer sea surface temperatures at the equator; therefore El Niño Southern Oscillation influences the variability of climate in the Pacific region and in Hawai‘i (Jin et al., 2014).

Tropical storm Wali was a storm event with precipitation >5.1 cm over a 24-hour period. The freshwater plume generated from Wali persisted in HFP for a period of 19 days, which is beyond the average recovery rates for HFP of 4 days. Wali occurred at the end of a neap tidal cycle going into a spring cycle, which should have led to increased flushing of the fishpond and aided a faster recovery time post Wali. Wind forcing is important in accelerating recovery rates, and in this case, the winds returned to average (~5m/s) within 3 days post-Wali. However, the salinity did not recover within HFP until the onset of strong winds brought by Iselle. Given that the flushing rates are fastest in the study area of the fishpond, relative to other areas of the fishpond, this particular storm may have had even longer-term impacts on the rest of the fishpond.

The quantity of rainfall and slow recovery rate for HFP following Wali suggests that the magnitude of the storm is significant for recovery time. Reduction in salinity by 1% during the same flood event caused a coral mortality event due to persistence of the freshwater plume in another area of Kāne‘ohe Bay affected by the Waiahole Stream estuary (Bahr 2015). Wali’s impacts on turbidity affect the water quality of the fishpond beyond recovery time. The chronic impact of sedimentation following a storm event is a mechanism for the process of sediment accumulation on the benthos of HFP. After the dramatic effects of the floods caused by Wali, as the double hurricanes (Iselle and Julio) approached Hawai‘i the pond managers installed boards across the mākāhā at RM2 and RM3 in an attempt to protect the fishpond from possible impact of another flood-storm event.

Tropical Storm Iselle was primarily characterized by strong winds (>15 m/s) in Kāne‘ohe Bay. Salinity, which was below average for the period following Wali, recovered to baseline conditions on August 8, during Iselle, possibly due to increased mixing of the water column due to high wind stress. Precipitation and stream discharge were not significant during Iselle.

Julio’s direct impacts were not significant at HFP however, the weather conditions created by the passing of the tropical storm were significant in HFP. During Julio the winds decreased by 27%

and further decreased by 177% during the days post Julio. The decrease in winds, in addition to the restricted flow from the barriers placed over the mākāhā, allowed the pond temperature to warm and caused stratification of the water column. Temperatures were on average 12% higher than normal post-Julio with values above 34 °C sustained during the day.

Management

Another factor that may have contributed to the recovery of salinity levels, during Iselle, may be due to the management of freshwater influx into HFP. Boarding the river mākāhā prevented freshwater input to the pond, therefore removing the dilution effect of seawater by freshwater. At the same time, the salinity recovered to levels closer to the range of seawater (average salinity = 28.692 PSU) due to decreased mixing with freshwater and perhaps in part to evaporation.

Warming of the internal temperature of the pond has had profound impacts in the past, with documented widespread fish kill events in HFP caused by sustained heat stress associated with reduction of wind stress due to El Niño conditions (McCoy et al., in prep.). During the fish kill events average temperatures reached 28 °C with daily maxima above 30 °C post-Julio. The temperatures at the study site were on average above 31 °C with daily maximums above 34 °C, which are well in excess of the environmental limit (McCoy et al., in prep.).

He‘eia Fishpond experienced the greatest increases in temperature during Tropical Storm Julio, during which time the pond mākāhā were boarded to reduce the storm impact. The greatest change in salinity occurred during Tropical Storm Wali, after substantial increases in both precipitation and stream discharge. It took the pond 19 days to recover from this event. Turbidity levels were most strongly affected by Tropical Storm Wali, and not the mangrove removal event as we had anticipated. Understanding how the environment responds to anthropogenic vs. natural events is critical for the proper management of the Fishpond environment. The physical characteristics of HFP make the conditions within HFP very sensitive to changes in water exchange through the mākāhā, which varies as a function of tidal stage and volume of stream discharge. The impacts of projected increases in sea surface temperatures due to global warming are expected to fuel an increased frequency of tropical storms in Hawai‘i (Murakami et al., 2013). It is important and historically significant that the exchange of freshwater through the river mākāhā are carefully regulated to mitigate the potential for future impacts due to climate variability.

APPENDIX

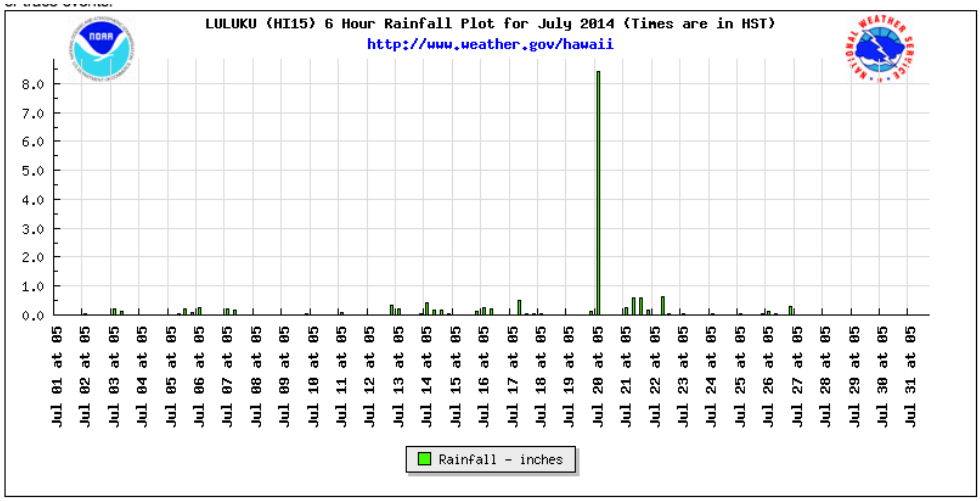

Appendix Figure 1. Luluku Rain Data for July (Luluku HI 15) for July 2014.

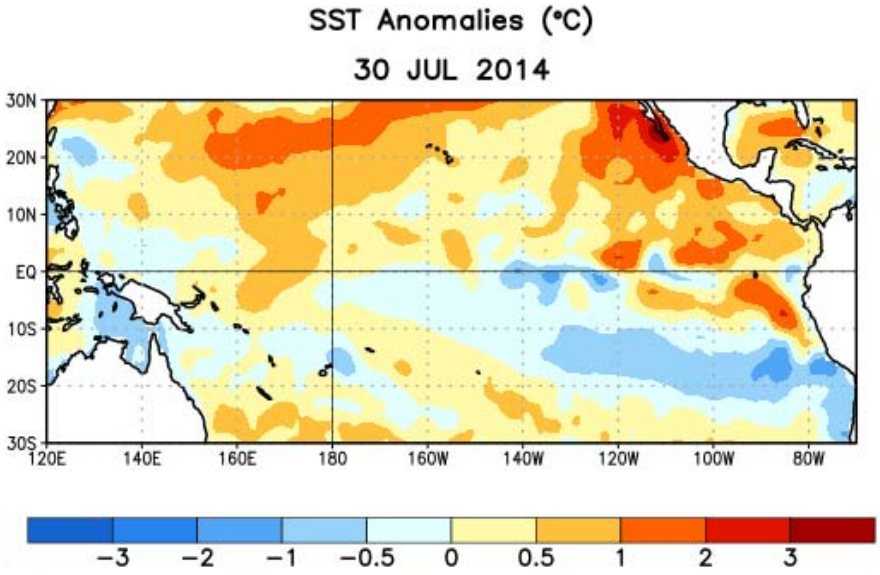

Appendix Figure 2. Average sea surface temperature (SST) anomalies (°C) for the week centered on 30 July 2014. Anomalies are computed with respect to the 1981-2010 base period weekly means. Figure and Caption: CLIMATE PREDICTION CENTER/NCEP/NWS and the International Research Institute for Climate and Society 7 August 2014.

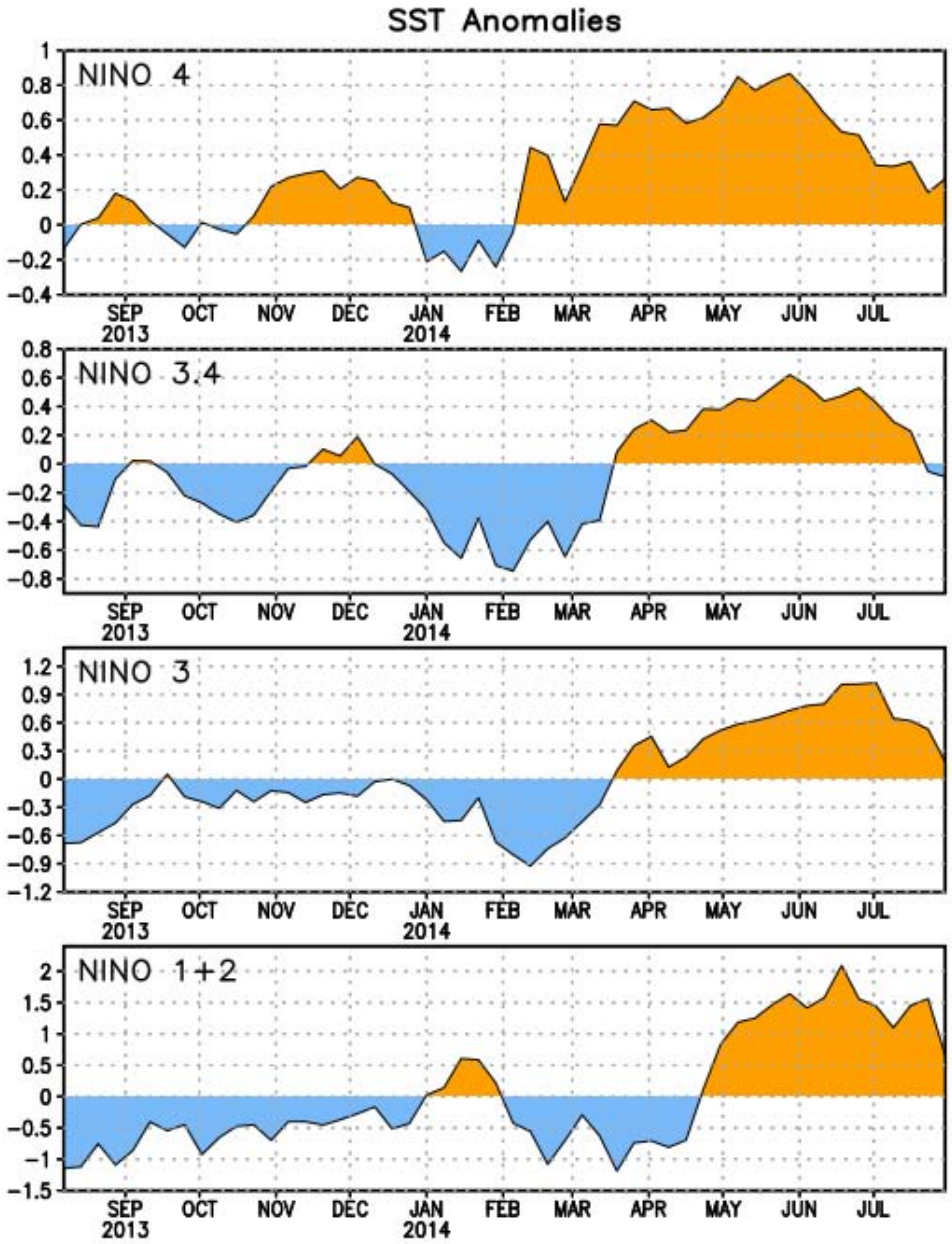

Appendix Figure 3. Time series of area-averaged sea surface temperature (SST) anomalies (°C) in the Niño regions [Niño-1+2 (0°-10°S, 90°W-80°W), Niño 3 (5°N-5°S, 150°W-90°W), Niño-3.4 (5°N-5°S, 170°W-120°W), Niño-4 (5ºN-5ºS , 150ºW-160ºE]. SST anomalies are departures from the 1981-2010 base period weekly means. Figure and Caption: CLIMATE PREDICTION CENTER/NCEP/NWS and the International Research Institute for Climate and Society 7 August 2014.

REFERENCES

D'Andrea, B. 2015. Water exchange and circulation in He'eia Fishpond: Building blocks for establishing a water budget. University of Hawai'i.

Devaney D., Kelly M., Jae Lee P., Motteler L. S.. 1976. Kāneʻohe A History of Change, 1976, Bishop Museum Press.

Demopoulos A.W. J., Craig R. Smith. 2010. Invasive mangroves alter macrofaunal community structure and facilitate opportunistic exotics, MARINE ECOLOGY PROGRESS SERIES, Vol. 404: 51–67.

Hoover, D. J., Mackenzie F. T.. 2009. Fluvial Fluxes of Water, Suspended Particulate Matter, and Nutrients and Potential Impacts on Tropical Coastal Water Biogeochmistry: Oʻahu, Hawaiʻi. Aquatic Geochemistry, 15:547-570.

Jokiel, P. L., Rodgers, K. S, Walsh, W. J., Polhemus, D. A., Wilhelm, T. A., Toonen, R J. 2011. Marine Resource Management in the Hawaiian Archipelago: The Traditional Hawaiian System in Relation to the Western Approach. Journal of Marine Biology, Vol. 2011.

Jin, F. -F. and Boucharel, J. and Lin, I. -I. 2014. Eastern Pacific tropical cyclones intensified by El Niño delivery of subsurface ocean heat. Nature 516:7529:82-85.

Keala, G., Hollyer, J.R., Castro, L., 2007. Loko Iʻa: A manual on Hawaiian fishpond restoration and management. College of Tropical Agriculture and Human Resources, University of Hawaii, Honolulu, 76 pp.

Kelly, M. 1975. *Loko Iʻa o Heʻeia*, Second ed. Bernice Pauahi Bishop Estate.

Kikuchi, W. 1976. Prehistoric Hawaiian Fishponds. Science 193, 295-299.

McCoy D., Alegado, R. A., McManus, M. A., Kotubetey, K., Kawelo, A. H., Young, C., Ruttenberg, K. C.. *In prep*. Large-scale climatic effects on a traditional Hawaiian fishpond . Environmental Research Letters.

Murakami H., Wang B., Li T., Kitoh A.. 2013. Projected increase in tropical cyclones near Hawaii. Nature Climate Change 3:749-754.

Ostrander, C. E., M. A. McManus, E. H. De Carlo, and F. T. Mackenzie. 2008. Temporal and spatial variability of freshwater plumes in a semi-enclosed estuarine-bay system. Estuaries and Coasts 31, 192-203.

Ringuet, S., Mackenzie, F. M., 2005. Controls on nutrient and phytoplankton dynamics during normal flow and storm runoff conditions, southern Kaneʻohe Bay, Hawaiʻi. Estuaries 28, 327-337.

Siple, Margaret C., Donahue, Megan J.. 2013. Invasive mangrove removal and recovery: Food web effects across a chronosequence, Journal of Experimental Marine Biology and Ecology, Vol.448, pp.128-135.

Timmerman A., Young C., McManus M.A., Ruttenberg K., Briggs R., D'Andrea B. *In Prep*. Dynamics of a culturally-significant, partially-enclosed tropical coastal system.

ONLINE REFERENCES

Google Earth. 2015. https://www.google.com/earth/

NOAA CLIMATE PREDICTION CENTER/NCEP/NWS and the International Research Institute for Climate and Society. 2014. EL NIÑO/SOUTHERN OSCILLATION (ENSO) DIAGNOSTIC DISCUSSION.
http://www.cpc.ncep.noaa.gov/products/expert_assessment/ENSO_DD_archive.shtml

NOAA National Data Buoy Center. Station MOKH1: 1612480 – Moku o Loe, HI. 2014.
http://www.ndbc.noaa.gov/station_page.php?station=mokh1

NOAA National Climatic Data Center. Rainfall Kāneʻohe 838.1. 2014.
https://www.ncdc.noaa.gov/cdo-web/

NOAA National Weather Service Forecast Office. LULUKU (HI15) Rainfall graphs. 2015.
http://www.prh.noaa.gov/hnl/hydro/pages/rra_graphs.php?station=LULH1&mo=072014

NOAA National Weather Service. Central Pacific Hurricane Center. Product Archive. 2014.
http://www.prh.noaa.gov/cphc/tcpages/archive.php

NOAA National Weather Service. Central Pacific Hurricane Center. Product Archive. Public Advisory. 2014.
http://www.prh.noaa.gov/cphc/tcpages/archive.php?stormid=CP012014

NOAA Tides and Currents. Moku o loe, HI - Station ID: 1612480. 2014.
http://tidesandcurrents.noaa.gov/stationhome.html?id=1612480

Paepae O Heʻeia. 2015. http://paepaeoheeia.org

USGS 16275000 Heʻeia Stream at Haiku Valley near Kāneʻohe, Oahu, HI, 2014.
http://waterdata.usgs.gov/hi/nwis/dvstat?referred_module=sw&search_site_no=16275000&format=sites_selection_links